

Received March 3, 2022, accepted March 21, 2022, date of publication March 25, 2022, date of current version March 31, 2022.

Digital Object Identifier 10.1109/ACCESS.2022.3162367

Dynamic Modeling and Solution of 6-DOF Parallel Mechanism

XUEDONG JING¹ AND CHENG LI²

¹School of Electrical and Electronic Engineering, Shanghai Institute of Technology, Shanghai 201416, China

²School of Mechanical Engineering, Shanghai Institute of Technology, Shanghai 201416, China

Corresponding author: Cheng Li (1446138357@qq.com)

This work was supported in part by the Science and Technology Commission of Shanghai Municipality under Grant 16090503700.

ABSTRACT When a parallel robot used in a scene that requires force control, rapid attitude adjustment, or precise positioning, we need to know the dynamic characteristics of the moving platform and the motion branch, so it is necessary to do the dynamic analysis of the parallel robot. In this study, for the six-degree-of-freedom parallel mechanism, the Newton-Eulerian method is used to model the dynamics, and then the inverse dynamics simulation is performed through the ADAMS simulation software to verify the correctness of the established dynamic equations. Finally, the Euler integration method is used to solve the dynamic equations numerically. When establishing dynamic equations, it is more convenient to use spiral coordinates to express the angular motion of the motion platform of the parallel mechanism. However, it is difficult to solve the equation numerically. When solving the equations in this study, Euler angles are used to express angular motion. The Euler angle is used as an iterative variable representing the angular motion in the solving process. Then the Euler angle is converted into a rotation matrix, and the parameters of the spiral coordinates are obtained through the rotation matrix, and the dynamic equation is finally solved. The simulation and calculation results show that the established dynamic equation is correct, and the solution to the dynamic equation is also correct.


INDEX TERMS Newton-Euler method, dynamic equations, Euler integration method, solution of the dynamic equation.

I. INTRODUCTION

Owing to the large load and high motion accuracy of parallel mechanisms, the application scenarios of parallel robots, such as satellite trackers [1], lifting mechanisms [2], and parallel machine tools [3], are becoming more and more extensive. However, it is crucial to accurately control the parallel robot during the application, analyze the dynamic characteristics of the manipulator, and model its dynamics. Many scholars have researched the dynamic modeling methods of parallel robots. The more classic methods include the Newton-Euler method, Lagrangian method, and virtual work principle [4].

The Newton-Euler method solves dynamics problems by establishing the force balance equation of each joint of the mechanism. In reference [5], the Newton-Euler method is used to analyze the dynamics of Hexarot parallel mechanisms and simulates them through ADAMS to verify the result. Reference [6] established the kinetic equation of the

3-PRRU parallel manipulator by the Newton-Euler method. Reference [7] proposed a dynamic modeling method for rigid-flexible mechanisms, in which the dynamic model of the Stewart platform was established using the Newton-Euler equation. In [8], the Newton-Euler method is used to model the dynamics of a six-degree-of-freedom parallel robot. The Lagrangian method is an energy-based dynamic method that eliminates all unwanted reaction forces. Therefore, this method is adopted by many people. In [9], pages 176-194 detail how to obtain the kinetic equations by the Lagrangian method. Reference [10] proposed a three-degree-of-freedom rope-driven parallel mechanism, established the dynamic equation of the mechanism by using the Lagrangian method and verified the correctness of the dynamic equation by combining Matlab numerical calculation and ADAMS simulation. Reference [11] analyzed the four degrees-of-freedom parallel manipulator's kinematics and working space and established a dynamics model through Lagrangian formulation. Reference [12] used the Lagrangian method to establish the dynamic equations of forging manipulators.

The associate editor coordinating the review of this manuscript and approving it for publication was Zheng H. Zhu .

Since the virtual work method does not need to calculate the binding force and moment, its calculation speed is faster than Newton's Euler method. Reference [13] performed an inverse kinetic analysis on the parallel platform applied to the NanShan Radio Telescope using a virtual work approach. Reference [14] analyzed the topological structure of the 3T1R parallel mechanism, modeled and analyzed the inverse dynamics of the space mechanism based on the principle of virtual work, and verified it by dynamic simulation with ADAMS software. Reference [15] Puglisi built a dynamic model for a 6 DOF hydraulic parallel robot based on the virtual work principle and then built a controller based on the model and performed a simulation. Reference [16] used the analysis method of the virtual work principle to model the dynamics of the 3-PUU parallel robot and compared the results of Matlab programming with the results of ADAMS dynamics simulation to verify the correctness of the dynamics model.

In addition to these classical dynamics modeling methods, [17] proposed an elastic dynamic modeling method for 6-RSS parallel robots. The method considers the elastic deformation of the branch chain and the clearance of the kinematic pair. Reference [18] proposed a systematic and modular dynamic modeling approach for parallel manipulators with complex limbs.

It is relatively easy to establish dynamic equations and calculate and simulate the inverse dynamics of the mechanism. However, it is more troublesome to do the forward dynamic analysis of the mechanism, that is, to solve the coupled second-order differential equations. Reference [19] using the decoupled natural orthogonal complement method and virtual spring method to analyze the forward dynamics of the parallel mechanism. In [20], the virtual work method is used to establish the dynamics equation of the 4RSS+PS parallel manipulator, and the inverse and forward dynamics are analyzed. In [21], forward dynamic analysis was performed on a 3-PRS parallel manipulator, and the influence of friction was considered.

In the above articles, only the method of establishing the dynamics model is introduced in the research on the dynamics of the six-degree-of-freedom parallel robot. The establishment of the dynamic equation is not verified, nor is the analysis of the forward dynamics. The kinetic equations are not validated, detrimental to precise experimental control later. Because when the experimental results are not ideal, we cannot determine whether the theoretical modeling is wrong or the experimental method is wrong. In addition, in terms of dynamics solution, forward dynamics analysis is crucial for the simulation of robots. In this study, the Newton-Eulerian method is used to model the dynamics of such parallel mechanisms. In order to facilitate the modeling, the angular motion of the moving platform is represented by spiral coordinates. Then the inverse dynamics simulation is performed through Adams simulation software, and the simulation results are compared with the calculation results of Matlab programming to verify the established dynamic

equations. The numerical solution of kinetic equations adopts the Euler iteration method, which is easy to understand and program. Euler angles represent angular motion when solving equations, convenient for iteration. Finally, through a numerical example, the calculation results are compared with the inverse dynamics inputs to verify the solution of the dynamic equation.

II. MODEL ANALYSIS

A. KINEMATIC ANALYSIS

The six-degree-of-freedom parallel mechanism based on Stewart is shown in Fig.1.

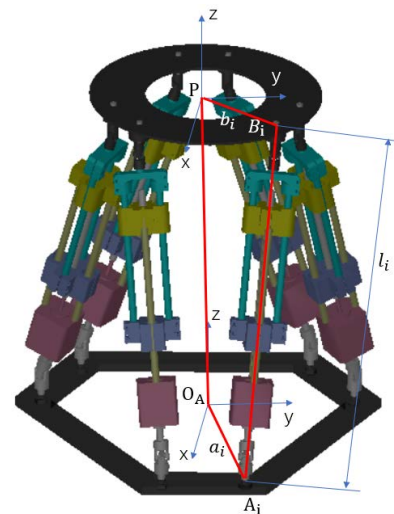


FIGURE 1. Six degrees of freedom parallel mechanism.

It includes a moving platform (upper platform), a static platform (lower platform), and six branch chains with the same structure. The Hooke hinge connects the static platform and the branch chain, and the moving platform and the branch chain are connected by the equivalent structure of the ball pair (the Hooke hinge plus a rotating pair).

The position and posture of the moving platform are changed by the expansion and contraction of the six branch chains. The coordinate system {A} of the lower platform is established on the center of the circumcircle of the lower platform, and the coordinate system {B} of the upper platform is established on the center of the circle of the upper platform. The initial postures of {A} and {B} are the same. The coordinates of the hinge point A_i of the lower platform on the static platform are represented by the vector a_i . The coordinates of the hinge point B_i of the upper platform on the moving platform are represented by the vector b_i .

According to this structure, the closed-loop kinematic equation of each branch can be obtained

$$l_i \hat{A} s_i + {}^A a_i = {}^A P + {}^A R_B {}^B b_i \quad (1)$$

where l_i is the length of the i -th branch chain, $\hat{A} s_i$ is the unit vector along the i -th branch chain in the coordinate system {A}, $i = 1, 2, \dots, 6$. P is the position vector of the center

point of the upper platform, and ${}^A R_B$ is the pose description for coordinate system {B} in the coordinate system {A}, ${}^B b_i$ represents the representation of the vector b_i in the coordinate system {B}.

Equation (1) can be written as

$$l_i \hat{A} s_i = {}^A P + {}^A R_B {}^B b_i - {}^A a_i \quad (2)$$

Multiplying both sides of the above equation by itself at the same time, the formula for calculating the length of each branch can be computed:

$$l_i^2 = [{}^A P + {}^A R_B {}^B b_i - {}^A a_i]^T [{}^A P + {}^A R_B {}^B b_i - {}^A a_i] \quad (3)$$

Differentiate both sides of equation (1) concerning the time at the same time

$${}^A v_p + {}^A \omega \times {}^A b_i = \dot{l}_i \hat{A} s_i + l_i ({}^A \omega_i \times \hat{A} s_i) \quad (4)$$

where ${}^A v_p$ is the velocity of the center point of the moving platform, ${}^A \omega$ is the angular velocity of the moving platform in the static coordinate system {A}, \dot{l}_i is the length change rate of the i-th branch chain, and ${}^A \omega_i$ is the angular velocity of the i-th branch chain, the \times symbol represents the cross product of two vectors.

The A in the upper left corner of equation (4) is omitted at simultaneously, and each vector is represented in the static coordinate system by default. Then, (4) can be written as

$$v_p + \omega \times b_i = \dot{l}_i \hat{s}_i + l_i (\omega_i \times \hat{s}_i) \quad (5)$$

Define the intermediate variable v_{b_i} as the velocity at point B_i :

$$v_{b_i} = v_p + \omega \times b_i \quad (6)$$

B. DYNAMIC ANALYSIS

The parallel mechanism is decomposed into an upper platform (moving platform), a lower platform (static platform), and six identical branch chains. Each branch chain is further divided into two parts: cylinder and piston.

Their force diagrams are shown in Fig. 2 and Fig. 3 (external disturbance forces and moments on the moving platform are not considered).

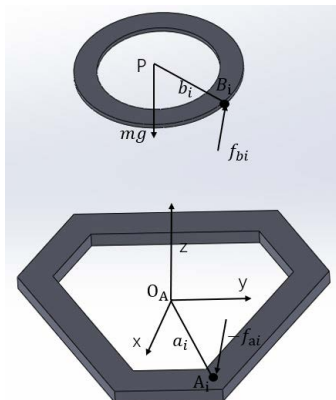


FIGURE 2. Force analysis diagram of the moving platform.

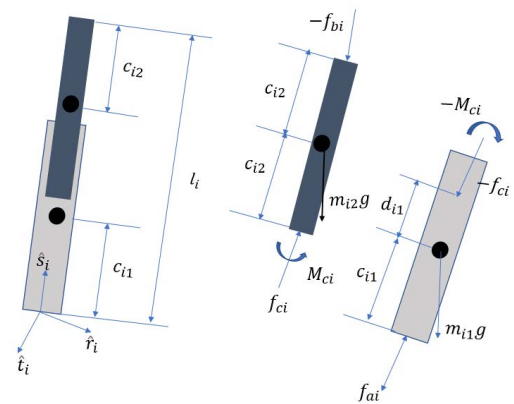


FIGURE 3. Branch chain force analysis diagram.

The Newton-Eulerian equations of the moving platform:

$$\sum F_{ext} = \sum_{i=1}^6 f_{bi} + mg = ma_p \quad (7)$$

$$\sum {}^p n_{ext} = \sum_{i=1}^6 b_i \times f_{bi} = {}^A I_p \dot{\omega} + \omega \times {}^A I_p \omega \quad (8)$$

where:

$${}^A I_p = {}^A R_B {}^B I_p {}^A R_B^T$$

Convert the Newton-Eulerian equations of the moving platform into closed-form kinetic equations:

$$M_P \ddot{\chi} + C_P \dot{\chi} + G_P = F_P \quad (9)$$

in which M_P denotes the upper platform mass matrix, C_P denotes the Coriolis and centrifugal matrix, G_P denotes the gravity vector, F_P denotes the force matrix, and

$$\chi = \begin{bmatrix} x_p \\ \theta \end{bmatrix}, \quad \dot{\chi} = \begin{bmatrix} v_p \\ \omega \end{bmatrix}, \quad \ddot{\chi} = \begin{bmatrix} a_p \\ \dot{\omega} \end{bmatrix}$$

$$M_P = \begin{bmatrix} mE_{3 \times 3} & 0_{3 \times 3} \\ 0_{3 \times 3} & {}^A I_p \end{bmatrix}_{6 \times 6},$$

$$C_P = \begin{bmatrix} 0_{3 \times 3} & 0_{3 \times 3} \\ 0_{3 \times 3} & \omega \times {}^A I_p \end{bmatrix}_{6 \times 6}$$

$$G_P = \begin{bmatrix} -mg \\ 0_{3 \times 1} \end{bmatrix}_{6 \times 1}, \quad F_P = \begin{bmatrix} \sum f_{bi} \\ \sum b_i \times f_{bi} \end{bmatrix}_{6 \times 1}$$

in which x_p, v_p, a_p represent linear motion of the moving platform, and $\theta, \omega, \dot{\omega}$ represent its angular motion. And $E_{3 \times 3}$ denotes 3×3 identity matrix, $0_{3 \times 3}$ denotes 3×3 zero matrix, and $0_{3 \times 1}$ denotes 3×1 zero vector.

The kinetic equation of the branched-chain:

The Newton-Eulerian equation of the cylinder part:

$$\sum F_{ext} = m_{i1} a_{i1} = f_{ai} - f_{ci} + m_{i1} g \quad (10)$$

$$\sum {}^{ci1} n_{ext} = {}^A I_{ci1} \dot{\omega}_i + \omega_i \times {}^A I_{ci1} \cdot \omega_i$$

$$= ci1 (-\hat{s} \times f_{ai}) + d_{i1} (\hat{s} \times -f_{ci}) - M_{ci} \quad (11)$$

where:

$$d_{i1} = l_i - c_{i1} - 2c_{i2}$$

$${}^A I_{ci1} = {}^A R_{A_i} {}^{A_i} I_{ci1} {}^A R_{A_i}^T$$

where $\sum F_{ext}$ is the sum of the external forces acting on the upper half of each branch, and $\sum^{ci1} n_{ext}$ is the external moment applied to the center of mass of the upper half of the branch.

The Newton-Eulerian equation of the piston part:

$$\sum F_{ext} = m_{i2} a_{i2} = f_{ci} - f_{bi} + m_{i2} g \quad (12)$$

$$\begin{aligned} \sum^{ci2} n_{ext} &= {}^A I_{ci2} \dot{\omega}_i + \omega_i \times {}^A I_{ci2} \cdot \omega_i \\ &= c_{i2} (-\hat{s} \times f_{ci}) + c_{i2} (\hat{s} \times -f_{bi}) - M_{ci} \end{aligned} \quad (13)$$

where:

$${}^A I_{ci2} = {}^A R_{A_i} {}^{A_i} I_{ci2} {}^A R_{A_i}^T$$

It can be seen from [22] that after simplification, the kinetic equation of the branch i can be written in the following form:

$$M_i \ddot{x}_i + C_i \dot{x}_i + G_i = F_i \quad (14)$$

where:

$$\begin{aligned} M_i &= m_{i2} \hat{s}_i \hat{s}_i^T - \frac{1}{l_i^2} I_{xxi} \hat{s}_{i \times}^2 - m_{ce} \hat{s}_{i \times}^2 \\ C_i &= -\frac{2}{l_i^2} m_{co} \hat{s}_i^T \dot{x}_i \hat{s}_{i \times}^2 - \frac{m_{i2} c_{i2}}{l_i^2} \hat{s}_i x_i^T \hat{s}_{i \times}^2 \\ G_i &= (m_{ge} \hat{s}_{i \times}^2 - m_{i2} \hat{s}_i \hat{s}_i^T) g \\ F_i &= -f_{bi} + \tau_i \hat{s}_i \end{aligned}$$

in which τ_i is the driving force of each branch.

To derive the closed-form dynamics of the entire platform, the intermediate generalized coordinate x_i (the position of point B_i) needs to be mapped to the main generalized coordinate χ . Using such a transformation, and the internal force f_{bi} can be eliminated. The intermediate generalized coordinates and the principal generalized coordinates are linked by defining the intermediate Jacobian matrix J_i .

Then, (6) can be written in the following form:

$$\dot{x}_i = J_i \dot{\chi} \quad (15)$$

where:

$$J_i = [E_{3 \times 3} \quad -b_{i \times}] \quad (16)$$

Equation (15) takes the time derivative:

$$\ddot{x}_i = J_i \ddot{\chi} + \dot{J}_i \dot{\chi} \quad (17)$$

Equation (16) takes the time derivative:

$$\begin{aligned} \dot{J}_i &= [0_{3 \times 3} \quad -((\omega \times b_i) \times E + b_{i \times} \dot{E})] \\ &= [0_{3 \times 3} \quad -\omega \times b_{i \times} + b_{i \times} \omega \times] \end{aligned}$$

Bring (15) and (17) into (14), and then multiply J_i^T on both sides of (14) to get

$$(J_i^T M_i J_i) \ddot{\chi} + (J_i^T M_i \dot{J}_i + J_i^T C_i J_i) \dot{\chi} + J_i^T G_i = J_i^T F_i \quad (18)$$

The above formula can be written in the following form

$$M_{li} \ddot{\chi} + C_{li} \dot{\chi} + G_{li} = F_{li} \quad (19)$$

where:

$$\begin{aligned} M_{li} &= J_i^T M_i J_i \\ C_{li} &= J_i^T M_i \dot{J}_i + J_i^T C_i J_i \\ G_{li} &= J_i^T G_i \\ F_{li} &= J_i^T F_i = \begin{bmatrix} I_{3 \times 3} \\ b_{i \times} \end{bmatrix} (-f_{bi} + \tau_i \hat{s}_i) \\ &= - \begin{bmatrix} f_{bi} \\ b_i \times f_{bi} \end{bmatrix} + \tau_i \begin{bmatrix} \hat{s}_i \\ b_i \times \hat{s}_i \end{bmatrix} \end{aligned}$$

Finally, the closed dynamic equation of the entire parallel mechanism is

$$M(\chi) \ddot{\chi} + C(\chi, \dot{\chi}) \dot{\chi} + G(\chi) = F \quad (20)$$

where:

$$M(\chi) = M_p + \sum_{i=1}^{i=6} M_{li} \quad (21a)$$

$$C(\chi, \dot{\chi}) = C_p + \sum_{i=1}^{i=6} C_{li} \quad (21b)$$

$$G(\chi) = G_p + \sum_{i=1}^{i=6} G_{li}$$

$$\begin{aligned} F &= J^T \tau \\ \chi &= \begin{bmatrix} x_p \\ \theta \end{bmatrix}; \dot{\chi} = \begin{bmatrix} v_p \\ \omega \end{bmatrix}; \ddot{\chi} = \begin{bmatrix} a_p \\ \dot{\omega} \end{bmatrix} \\ x^p &= [x \quad y \quad z] \\ \theta &= t\heta [sx \quad sy \quad sz] \\ v^p &= [\dot{x} \quad \dot{y} \quad \dot{z}] \\ \omega &= \omega [sx \quad sy \quad sz] \\ a^p &= [\ddot{x} \quad \ddot{y} \quad \ddot{z}] \\ \dot{\omega} &= \omega ad \cdot [sx \quad sy \quad sz] \end{aligned} \quad (21c)$$

in which $t\heta$ denotes the rotation angle of the angular motion of the moving platform, ω denotes its angular velocity, ωad denotes its angular acceleration, and $[sx \ sy \ sz]$ denotes the rotation axis of its angular motion.

When doing inverse dynamics analysis, the driving force τ of the branch chain is obtained according to the motion trajectory of the moving platform.

Equation (20) can be rewritten as

$$\tau = J^{-T} [M(\chi) \ddot{\chi} + C(\chi, \dot{\chi}) \dot{\chi} + G(\chi)] \quad (22)$$

III. VALIDATION OF DYNAMIC EQUATIONS

Before solving the dynamic equation, the correctness of the established dynamic equation should be verified. The Adams virtual prototype model is verified by comparing the inverse kinematics simulation of ADAMS with the inverse kinematics calculation results of Matlab. By comparing the inverse dynamics simulation of the ADAMS model with the inverse dynamics calculation results of Matlab, the established dynamics model is verified.

A. KINEMATICS SIMULATION

A model of a six-degree-of-freedom parallel platform was established in SolidWorks, imported into Adams [23], and the

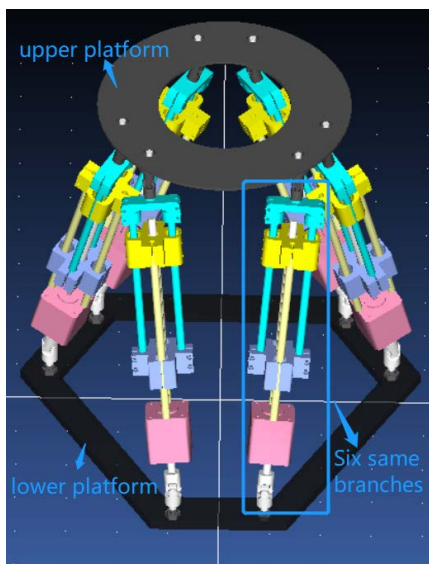


FIGURE 4. Adams simulation model.

required constraints were added. The final virtual prototype model is shown in Fig. 4.

Applying a General Point Motion at the center of mass of the upper platform of the model can realize the motion of 6 degrees of freedom in space, as shown in Fig. 5. Select a point on the ground or the static platform for the Reference Point, set the Type to displacement and the motion equation. The motion added to the center of mass of the upper platform is a sinusoidal motion with an amplitude of 5mm and a frequency of 1Hz along the Z direction. The function expression is:

$$z = A \sin(\omega t + \varphi) = 5 * \sin(2 * \pi * t) \quad (23)$$

Set the simulation End time to a motion cycle of 1s, and set the simulation Steps to 100 steps. Select the upper hinge center point to the lower hinge center point to establish a point-to-point measurement. Because it is a sinusoidal application

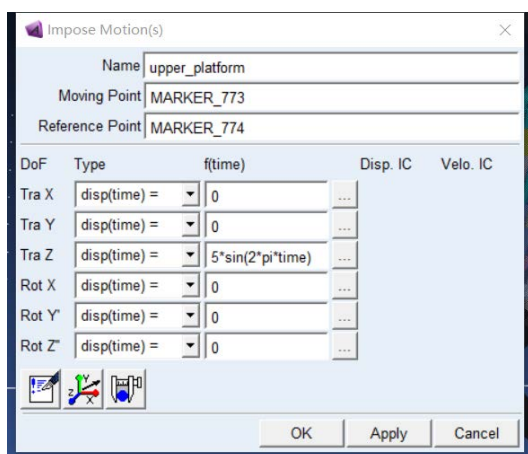


FIGURE 5. Apply point motion at the center of mass of the moving.

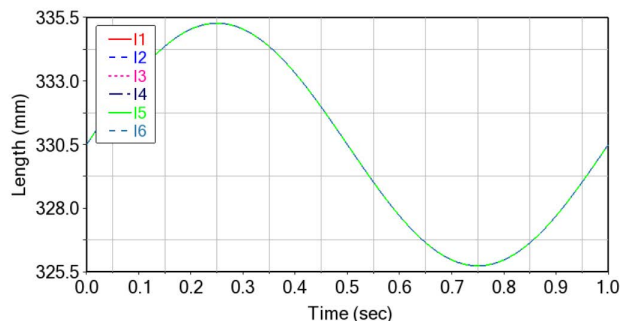


FIGURE 6. Length curves of 6 branch chains for kinematic simulation.

along the z-axis, as shown in Fig. 6, the length of the six chains changes the same over time.

In order to verify the correctness of the simulation model, the structural parameters and kinematic functions of the simulation model are brought into the theoretical model of the inverse kinematics solution, and the chain length change curve is obtained as shown in Fig. 7.

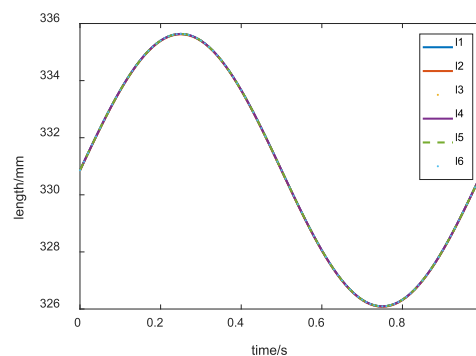


FIGURE 7. Variation curve of branch chain length calculated by Matlab.

The error curve is obtained by comparing the different results of the branch length variations obtained by Matlab programming with the simulation results, as shown in Fig. 8. It can be seen that the chain length error is in the magnitude of $10^{-1}mm$, indicating that the virtual prototype model is correct.

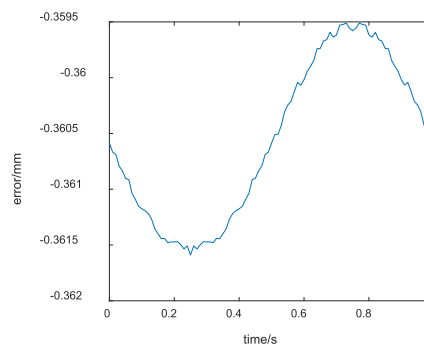


FIGURE 8. Error curve for chain length variation.

B. DYNAMIC SIMULATION

The length variation curves of the six branch chains obtained by the simulation in the previous section are added as spline functions in sequence. In the Post-Processor module, select the curve and select the Create Spline button to get six spline functions: SPLINE_1~SPLINE_6. Then set the point drive added on the moving platform to Deactivate, and add the moving drive MOTION_1~MOTION_6 on the moving pair of each branch chain. Set the drive function of each drive as AKISPL(time, 0, SPLINE_1, 0), . . . , AKISPL(time, 0, SPLINE_6, 0), as shown in Fig. 9.

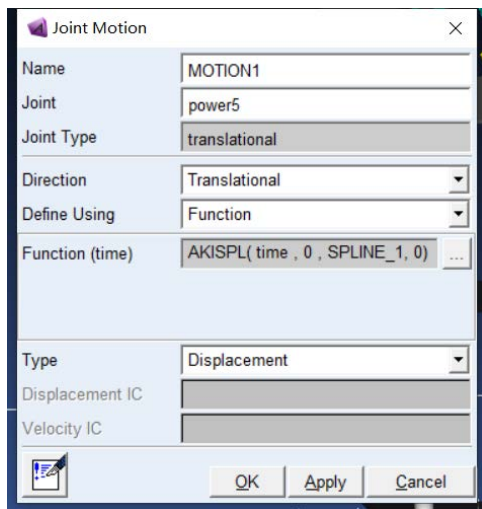


FIGURE 9. Set the driver function.

Add a force measurement to each drive, set the simulation time to 1s, step size to 100, run the simulation, and get the driving force required for the moving platform to generate the corresponding motion, as shown in Fig. 10. It can be seen from the Fig.10 that the driving force fluctuates slightly at 0.5s and 1s, and the position of the moving platform at these two times is the same as the starting position. The reason for the fluctuation is that during assembly, the starting position of the moving platform does not coincide with the lower platform in the x and y directions. The displacement function (23) of the upper platform, the first-order derivative (velocity function) and the second-order derivative (acceleration function) of the displacement function are brought into the inverse dynamic expression (22). The driving force results calculated by programming in Matlab are shown in Fig. 11. Comparing the two driving forces, the error curve of the driving force can be obtained, as shown in Fig. 12.

It can be seen from the driving force error curve that the simulation results are the same as the theoretical calculation results, and the driving force error is in the magnitude of $10^{-2}N$. Therefore, it can be proved that the dynamic model established according to the parallel mechanism in this paper is correct.

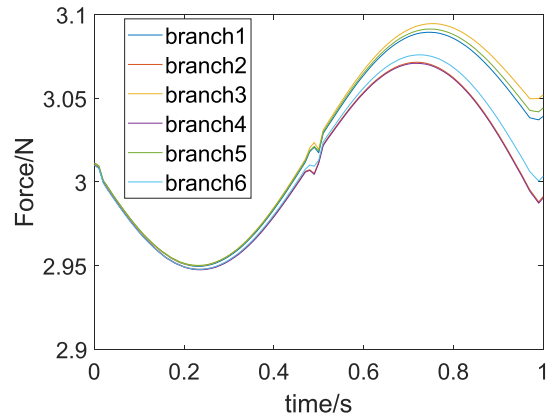


FIGURE 10. Driving force simulation results of each branch chain in Adams.

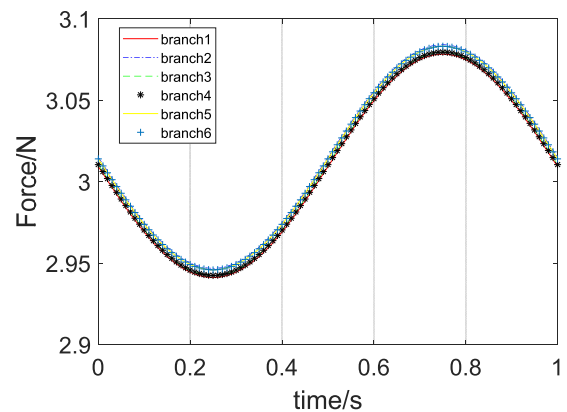


FIGURE 11. The driving force of each branch calculated by Matlab.

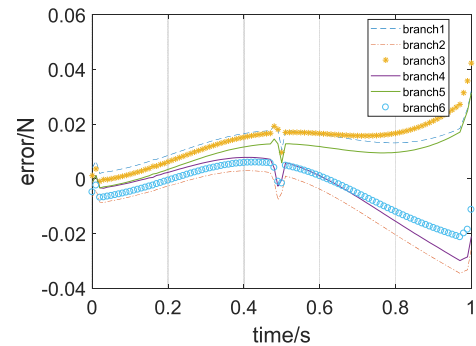


FIGURE 12. Driving force error curve of each branch.

IV. SOLVE DYNAMIC EQUATION

Solving the dynamic equation is to do the forward dynamic analysis of the parallel mechanism, knowing the driving force of each branch chain, and solving the displacement, velocity, and acceleration of the moving platform.

A. METHOD

Equation (20) can be written in the following form:

$$\ddot{\chi} = M(\chi)^{-1} [F - C(\chi, \dot{\chi}) \dot{\chi} - G(\chi)] \quad (24)$$

When time $t = 0$

$$\chi(0) = \chi_0 \quad \dot{\chi}(0) = 0$$

Substitute $\chi(0)$ and $\dot{\chi}(0)$ into (24) to obtain $\ddot{\chi}(0)$, and then use the obtained $\ddot{\chi}(0)$ for the following calculation of χ and $\dot{\chi}$.

The iterative process is as follows:

$$\dot{\chi}(t + \Delta t) = \dot{\chi}(t) + \ddot{\chi}(t) \Delta t \tag{25}$$

$$\chi(t + \Delta t) = \chi(t) + \dot{\chi}(t) \Delta t + \frac{1}{2} \ddot{\chi}(t) \Delta t^2 \tag{26}$$

Since helical coordinates represent the angular motion of the motion platform during dynamic modeling, its components in the x, y, and z directions are not independent. They are composed of two variables, so it is not suitable for iteration. Therefore, in forwarding dynamics analysis, the Euler angles are used to describe the angular motion of the moving platform and as the iterative variables. The calculation process is shown in Fig. 13.

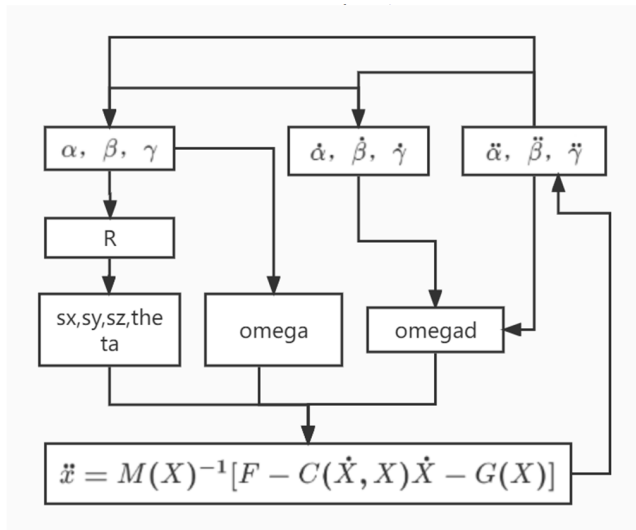


FIGURE 13. Dynamic equation solving flow chart.

$\theta, \omega, \dot{\omega}$ can be written as

$$\begin{aligned} \theta &= [\alpha \quad \beta \quad \gamma] \\ \omega &= [\dot{\alpha} \quad \dot{\beta} \quad \dot{\gamma}] \\ \dot{\omega} &= [\ddot{\alpha} \quad \ddot{\beta} \quad \ddot{\gamma}] \end{aligned}$$

Then, (25) can be written as

$$\begin{cases} \dot{x}(t + \Delta t) = \dot{x}(t) + \ddot{x}(t) \Delta t \\ \dot{y}(t + \Delta t) = \dot{y}(t) + \ddot{y}(t) \Delta t \\ \dot{z}(t + \Delta t) = \dot{z}(t) + \ddot{z}(t) \Delta t \\ \dot{\alpha}(t + \Delta t) = \dot{\alpha}(t) + \ddot{\alpha}(t) \Delta t \\ \dot{\beta}(t + \Delta t) = \dot{\beta}(t) + \ddot{\beta}(t) \Delta t \\ \dot{\gamma}(t + \Delta t) = \dot{\gamma}(t) + \ddot{\gamma}(t) \Delta t \end{cases}$$

$$\begin{cases} x(t + \Delta t) = x(t) + \dot{x}(t) \Delta t + \frac{1}{2} \ddot{x}(t) \Delta t^2 \\ y(t + \Delta t) = y(t) + \dot{y}(t) \Delta t + \frac{1}{2} \ddot{y}(t) \Delta t^2 \\ z(t + \Delta t) = z(t) + \dot{z}(t) \Delta t + \frac{1}{2} \ddot{z}(t) \Delta t^2 \\ \alpha(t + \Delta t) = \alpha(t) + \dot{\alpha}(t) \Delta t + \frac{1}{2} \ddot{\alpha}(t) \Delta t^2 \\ \beta(t + \Delta t) = \beta(t) + \dot{\beta}(t) \Delta t + \frac{1}{2} \ddot{\beta}(t) \Delta t^2 \\ \gamma(t + \Delta t) = \gamma(t) + \dot{\gamma}(t) \Delta t + \frac{1}{2} \ddot{\gamma}(t) \Delta t^2 \end{cases}$$

The programming process in Matlab is as follows:

1. the known a, b, c in the initial state of the moving platform.
2. Calculate the rotation matrix R by Euler angles.
3. Calculate the first derivative ω of θ and the helical coordinate parameters s_x, s_y, s_z, θ by the rotation matrix R.
4. Calculate $\ddot{\alpha}, \ddot{\beta}, \ddot{\gamma}$ by (21).
5. Calculate the second derivative ω_{ad} of θ .
6. Solve for $\ddot{\alpha}, \ddot{\beta}, \ddot{\gamma}$ by (24).
7. Calculate the new values of χ and $\dot{\chi}$ by (25) and (26).
8. Go to step 2.

B. AN EXAMPLE

First, given the desired trajectory, the driving force required by the desired trajectory is calculated through inverse dynamics. This driving force is then brought into the dynamic equation, and the trajectory of the moving platform is calculated by the Euler integration method. Compare the calculated trajectory with the given trajectory to verify the correctness of the solution method.

The calculation example in this paper is to plan a cubic polynomial trajectory, which includes both rotation and translation, and the initial and final velocities are 0. That is, the center of mass of the moving platform moves 30mm along the z-axis within 1s, and at the same time rotates 10° around the x-axis.

The trajectory expression is

$$z(t) = 382.5 + 90t^2 - 60t^3 \tag{27}$$

$$\begin{cases} s_x = 1, s_y = 0, s_z = 0 \\ \theta = \pi/6t^2 - \pi/9t^3 \end{cases} \tag{28}$$

The above two equations are brought into (22), and the driving force τ of each branch chain can be obtained through inverse dynamics calculation. Taking τ as the input of forwarding dynamics analysis, the time-varying curve of the motion trajectory of the moving platform is obtained. Compare the results calculated by the forward dynamics with the trajectory given by the reverse dynamics, as shown in Fig. 14 and Fig. 15.

As shown in Fig. 14, the calculation result of the translation direction is consistent with the given trajectory. From Fig. 15, we can see that the error between the calculation result of the rotation direction and the given trajectory increases in

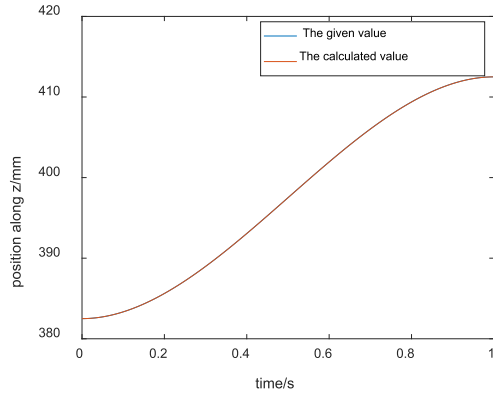


FIGURE 14. The given position and the calculated position of the moving platform.

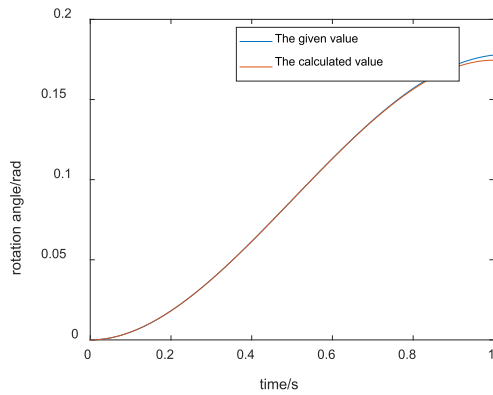


FIGURE 15. The given attitude and the calculated attitude of the moving platform.

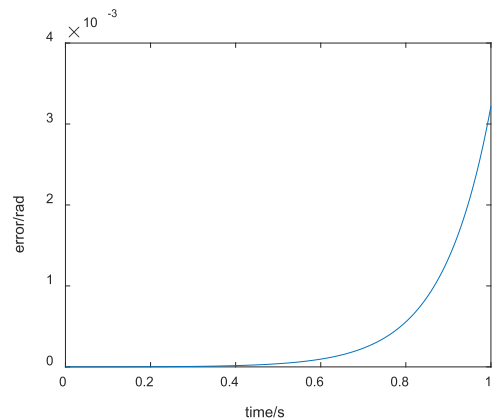


FIGURE 16. Error in rotation around the x-axis.

the period of 0.8s-1s. But from the error curve in Fig. 16, we can see that this error is within an acceptable range. If we want to reduce the error, we can set a smaller step size, but the calculation time will increase accordingly. Therefore, this paper selects a step with a shorter calculation time and the calculation result is within the acceptable range.

From the error plots in the rotational and translational directions, as shown in Fig. 17 and Fig. 18, we can see that

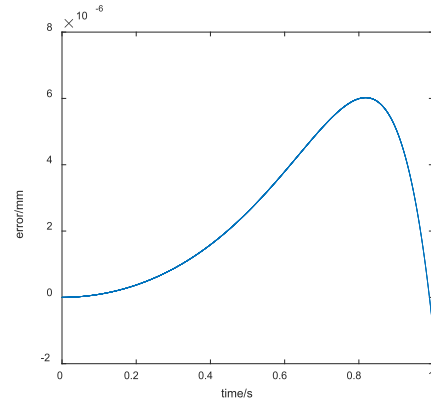


FIGURE 17. Error in translation along the z-axis.

the calculated error is acceptable. Therefore, the dynamics solution method in this paper is correct.

V. CONCLUSION

This paper uses the Newton Euler method to establish the dynamic model of the six-degree-of-freedom parallel mechanism, uses the ADAMS simulation software to do inverse dynamic analysis, and compares it with the calculation results of Matlab to verify the correctness of the dynamic model. Then, the Euler integration method is used to analyze the forward dynamics of the parallel mechanism. Euler angles represent the attitude of the moving platform. During the solution process, Euler angles are used as iterative variables. Finally, the method is verified by numerical examples. The work of this paper combines the convenience of establishing dynamic equations with helical coordinates and the easy-to-understand and easy-to-program properties of Euler integration in solving dynamic equations.

APPENDIX

TABLE 1. Geometric and inertial parameters of parallel mechanisms.

Symbol	Quantity	Value
m	upper platform quality	0.815kg
g	gravity	9806mm/s ²
m_{i1}	cylinder mass	0.88kg
m_{i2}	piston mass	0.14kg
c_{i1}	The distance between the center of mass of the cylinder and the point of force	90mm
c_{i2}	The distance between the center of mass of the piston and the point of force	111mm
I_{xxi}	Moment of inertia of the branch chain around the x axis	3786kg · mm ²

Coefficients in Equation (14)

$$m_{ce} = \frac{2}{l_i^2} (m_{i1}c_{i1}^2 + m_{i2}c_{i2}^2)$$

$$m_{co} = \frac{1}{l_i} m_{i2} c_{i2} - \frac{1}{l_i^2} (I_{xxi} + l_i^2 m_{ce})$$

$$m_{ge} = \frac{1}{l_i} (c_{i1} m_{i1} + m_{i2} (l_i - c_{i2}))$$

Jacobian Matrix for Parallel Platforms

$$J^T = \begin{bmatrix} \hat{s}_1 & \hat{s}_2 & \cdots & \hat{s}_6 \\ b_1 \times \hat{s}_1 & b_2 \times \hat{s}_2 & \cdots & b_6 \times \hat{s}_6 \end{bmatrix}$$

Inertia matrix of the moving platform

$$I_p = \begin{bmatrix} 4038 & 0 & 0 \\ 0 & 4038 & 0 \\ 0 & 0 & 8076 \end{bmatrix}$$

The position of the hinge point of the moving platform

$$B1 = [73.20508076, -73.20508076, -36.5];$$

$$B2 = [-73.0508076, -73.20508076, -36.5];$$

$$B3 = [-100, -26.79491924, -36.5];$$

$$B4 = [-26.79491924, 100, -36.5];$$

$$B5 = [26.79491924, 100, -36.5];$$

$$B6 = [100, -26.79491924, -36.5];$$

Static platform hinge point position

$$A1 = [45, -167.94228634, 30.25];$$

$$A2 = [-45, -167.94228634, 30.25];$$

$$A3 = [-167.94228634, 45, 30.25];$$

$$A4 = [-122.94228634, 122.94228634, 30.25];$$

$$A5 = [122.94228634, 122.94228634, 30.25];$$

$$A6 = [167.94228634, 45, 30.25];$$

REFERENCES

- [1] Y. D. Patel and P. M. George, "Parallel manipulators applications—A survey," *Mod. Mech. Eng.*, vol. 2, no. 3, pp. 57–64, Apr. 2012.
- [2] J. Jiang, D. Wu, T. He, Y. Zhang, C. Li, and H. Sun, "Kinematic analysis and energy saving optimization design of parallel lifting mechanism for stereoscopic parking robot," *Energy Rep.*, vol. 8, pp. 2163–2178, Nov. 2022.
- [3] W. A. N. G. Liping, K. O. N. G. Xiangyu, and Y. U. Guang, "Motor servo control parameter tuning for parallel and hybrid machine tools based on a genetic algorithm," *J. Tsinghua Univ. Sci. Techn.*, vol. 61, no. 10, pp. 1106–1114, 2022, doi: 10.16511/j.cnki.qhdxxb.2021.22.009.
- [4] D. Li, "Dynamic modeling and compliance control strategy of Stewart parallel robot," M.S. thesis, Dept. Obstetrics Gynecol., Jilin Univ., Jilin, China, 2021.
- [5] S. Pedrammehr, B. Danaei, H. Abdi, M. T. Masouleh, and S. Nahavandi, "Dynamic analysis of hexarot: Axis-symmetric parallel manipulator," *Robotica*, vol. 36, no. 2, pp. 225–240, Feb. 2018, doi: 10.1017/S0263574717000315.
- [6] G. Chen, W. Yu, Q. Li, and H. Wang, "Dynamic modeling and performance analysis of the 3-PRR 1T2R parallel manipulator without parasitic motion," *Nonlinear Dyn.*, vol. 90, no. 1, pp. 339–353, Jul. 2017.
- [7] B. Zi, B. Y. Duan, J. L. Du, and H. Bao, "A dynamic modeling method for the combination of FAST cable-driven parallel robot and stewart platform," *J. Tsinghua Univ. Sci. Techn.*, vol. 18, pp. 1–8, Jan. 2022, doi: 10.16511/j.cnki.qhdxxb.2021.26.039.
- [8] W. Khalil, "Dynamic modeling of robots using NewtonEuler formulation," *Informati. Contr. Autom. Robot.*, vol. 89, no. 1, pp. 3–20, 2011, doi: 10.1007/978-3-642-19539-6_1.
- [9] M. W. Spong, S. Hutchinson, and M. Vidyasagar, "Dynamics," in *Robot Modeling and Control*, 12nd ed. Hoboken, NJ, USA: Wiley, ch. 6, sec. 2, pp. 176–194.
- [10] W. Zhu, K. Shi, Y. Wang, H. Sen, and E. Duan, "Optimization design of 3-DOFs translational cable-driven rigid-flexible hybrid parallel mechanism and its dynamics analysis," *Trans. Chin. Soc. Agricult. Machinery*, vol. 52, no. 12, pp. 417–425, Dec. 2021.
- [11] O. Altuzarra, A. Zubizarreta, I. Cabanes, and C. Pinto, "Dynamics of a four degrees-of-freedom parallel manipulator with parallelogram joints," *Mechatronics*, vol. 19, no. 8, pp. 1269–1279, Dec. 2009, doi: 10.1016/j.mechatronics.2009.08.003.
- [12] W.-H. Ding, H. Deng, Q.-M. Li, and Y.-M. Xia, "Control-orientated dynamic modeling of forging manipulators with multi-closed kinematic chains," *Robot. Comput. Integr. Manuf.*, vol. 30, no. 5, pp. 421–431, Oct. 2014, doi: 10.1016/j.rcim.2014.01.003.
- [13] G. Kazezkhan, B. Xiang, N. Wang, and A. Yusup, "Dynamic modeling of the stewart platform for the NanShan radio telescope," *Adv. Mech. Eng.*, vol. 12, no. 7, Jul. 2020, Art. no. 168781402094007, doi: 10.1177/1687814020940072.
- [14] H. U. A. N. G. Kaiwei, S. H. E. N. Huiping, L. I. Ju, Z. H. U. Zhongqi, and Y. A. N. G. Tingli, "Topological design and dynamics modeling of a spatial 2T1R parallel mechanism with partially motion decoupling and symbolic forward kinematics," *China Mech. Eng.*, vol. 33, no. 2, pp. 160–169, Jan. 2022.
- [15] L. J. Puglisi, "Advanced control strategies for a 6 DOF hydraulic parallel robot based on the dynamic model," Ph.D. dissertation, Dept. Automat., Elect. Electron. Eng. Ind. Inform., Autom. Robot., Techn. Univ. Madrid, Madrid, Spain, 2016.
- [16] J. W. Mou, "Research on dynamic modeling and control strategy of 3-PUU parallel robot," M.S. thesis, School Mech. Eng., Chongqing Univ., Chongqing, China, 2017.
- [17] L. Wang, B. Xu, M. Zheng, Z. Zhu, and D. Zhang, "Elastic dynamics modeling and analysis for a 6-RSS parallel robot with joint clearance," *Comput. Integr. Manuf. Syst.*, to be published. [Online]. Available: <http://kns.cnki.net/kcms/detail/11.5946.tp.20211228.1404.018.html>
- [18] A. Müller, "Dynamics of parallel manipulators with hybrid complex limbs—Modular modeling and parallel computing," *Mechanism Mach. Theory*, vol. 167, Jan. 2022, Art. no. 104549.
- [19] A. Raoofian, A. E. Kamali, and A. Taghvaeipour, "Forward dynamic analysis of parallel robots using modified decoupled natural orthogonal complement method," *Mechanism Mach. Theory*, vol. 115, pp. 197–217, Sep. 2017, doi: 10.1016/j.mechmachtheory.2017.05.002.
- [20] S. Zarkandi, "Inverse and forward dynamics of a 4 R SS+ PS parallel manipulator with one infinite rotational motion," *Austral. J. Mech. Eng.*, vol. 20, pp. 1–19, Jan. 2020, doi: 10.1080/14484846.2020.1714352.
- [21] W.-H. Yuan and M.-S. Tsai, "A novel approach for forward dynamic analysis of 3-PRS parallel manipulator with consideration of friction effect," *Robot. Comput.-Integr. Manuf.*, vol. 30, no. 3, pp. 315–325, Jun. 2014, doi: 10.1016/j.rcim.2013.10.009.
- [22] H. D. Taghirad, "Dynamics," in *Parallel Robots: Mechanics and Control*, 12nd ed. Boca Raton, FL, USA: CRC Press, 2018, ch. 5, sec. 3, pp. 199–210.
- [23] Z. G. Li, *ADAMS Entry Details and Examples*, 2nd ed. Beijing, China: National Defence Industry Press, 2014, ch. 2, sec. 3, pp. 49–58.



XUEDONG JING received the B.S. and M.S. degrees in mechanical engineering from the Shaanxi University of Science and Technology, Shaanxi, China, in 1991 and 1999, respectively, and the Ph.D. degree from Shanghai Jiao Tong University, Shanghai, China, in 2000. He is now a Professor and the Dean of the School of Electrical and Electronic Engineering, Shanghai Institute of Technology, Shanghai. His research interests include robotics and virtual instrument technology.



CHENG LI was born in Henan, China, in 1997. He received the B.S. degree in mechanical engineering from Beihua University, in 2019. He is currently pursuing the M.S. degree with the School of Mechanical Engineering, Shanghai Institute of Technology, Shanghai, China. His research interest includes parallel robot.

...